Stability of Hydrophobically Modified Poly(*p*-phenylenesulfonate) Bundles As Observed by Molecular Dynamics Simulation

Berk Hess,*,† Mehmet Sayar,‡ and Christian Holm†,§

Max-Planck-Institut für Polymerforschung, Mainz, Germany; Koc University, College of Engineering, Istanbul, Turkey; and Frankfurt Inst. for Advanced Studies, J.W. Goethe-Universität, Frankfurt, Germany

Received November 15, 2006; Revised Manuscript Received January 3, 2007

ABSTRACT: The bundle formation in solution of hydrophobically modified sulfonated poly(*p*-phenylene) oligomers (PPP) is studied by molecular dynamics simulations. These oligomers form cylindrical micelles in water. Light scattering experiments suggest that the number of PPP oligomers in the cross section is around 10−19 when monovalent Na^+ is used as counterion. On the other hand, if divalent Ca^{2+} counterions are used, this number dramatically increases to 60 oligomers. Here, we show that the basic packing of the PPP oligomers does not change upon increase of the counterion valency. However, the interaction among bundles goes from repulsive to attractive as the counterions are changed from Na^+ to Ca^{2+}. We propose that the observed aggregate size of 60 oligomers could be explained by aggregation of several bundles (i.e., bundle of bundles).

I. Introduction

Attractive interactions among like-charged polyelectrolytes have drawn a lot of attention in the past decades. This phenomenon has unique implications for our understanding of the structure and function of biopolymers, such as DNA and proteins, and also has a significant technological importance for its role in designing self-assembling nanosystems. The origin of the attractive interactions has been well studied in several experimental and theoretical studies.[1−4] Biological systems provide several examples with different morphologies. The aggregation of DNA in the presence of multivalent counterions,[5] assembly of F-actin,[6,7] and microtubules[6] into bundle like aggregates are some of the well-known and well-studied examples. The origin of the attraction among like-charged polyelectrolytes is short-range ionic correlations of multivalent counterions.[1−4] This phenomenon cannot be explained on a mean-field level. However, in recent years, several theoretical and computational studies, which take into account the correlations of the counterions, have provided us with a good understanding of the underlying mechanisms, although some questions, especialy related to bundeling of polyelectrolytes in the presence of multivalent counterions, are not sufficiently settled.[8]

Model synthetic systems can be used to extend our understanding of the detailed balance which enables formation of finite and well-defined aggregates. These model systems enable a controlled tuning of the parameters and analysis of the contribution from several different aspects of the system. Hydrophobically modified sulfonated poly(*p*-phenylene) (PPP) provides a good example for such model systems (Figure 1).[9,10] The basic repeat unit is composed of three phenyl rings, where two of the rings carry SO_3^- charged groups and the third group carries a hydrophobic side chain composed of a short alkyl, $C_{12}H_{25}$. In experiments PPP oligomers are usually composed of 20−40 repeat units. The neutralizing counterions are either monovalent Na^+ or divalent Ca^{2+}. In dilute solutions these systems form cylindrical aggregates with a length of roughly half a micron. The core of the cylinder is composed of hydrophobic side chains, whereas the charged groups are distributed on the surface of this cylindrical aggregate. Light scattering experiments reveal the radial aggregation number (number of oligomers in the cross section) as 10−19 oligomers and the axial aggregation number as 4−5 oligomers in the presence of monovalent counterions. Exchange of the monovalent counterions with divalent Ca^{2+} leads to a surprising increase in the aggregation number to ≈60 oligomers.[11] Considering the short length of the hydrophobic side chains, such a high number of oligomers cannot be packed into a circular cross section without creating a cavity in the center. A cavity in the center would require water molecules to fill up the void, which would lead to an unfavorable contact surface between the hydrophobic side chains and the water molecules.

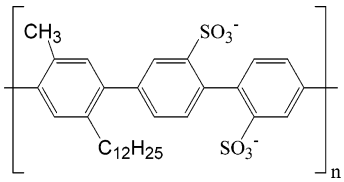

Figure 1. Hydrophobically modified sulfonated PPP oligomers.

The aggregation of hydrophobically modified PPP oligomers in the presence of Na^+ counterions has already been studied via a coarse-grained model of the PPP oligomers.[12,13] In these systems the balance of the attractive hydrophobic interactions, the repulsive electrostatic interactions among backbone monomers, and the counterion entropy determines the bundle size. These systems demonstrate a nonmonotonic dependence on the strength of the electrostatic interactions. In high dielectric constant solvents, most of the counterions are free in solution, and the aggregates are highly charged. On the other extreme of a very low dielectric constant, most counterions are condensed, leading to almost a neutral aggregate. These charged rods with hydrophobic attractions are also closely linked to the Rayleigh charged hydrophobic droplet. This problem has been studied by Deserno[14] for a charged droplet and by Tamashiro and Schiessel[15] for charged cylinders, within mean-field approximation. Deserno has demonstrated that the droplet size is always

* To whom correspondence should be addressed.
† Max-Planck-Institut für Polymerforschung.
‡ Koc University, College of Engineering.
§ J.W. Goethe-Universität.

10.1021/ma062624g CCC: $37.00
Published on Web 02/06/2007

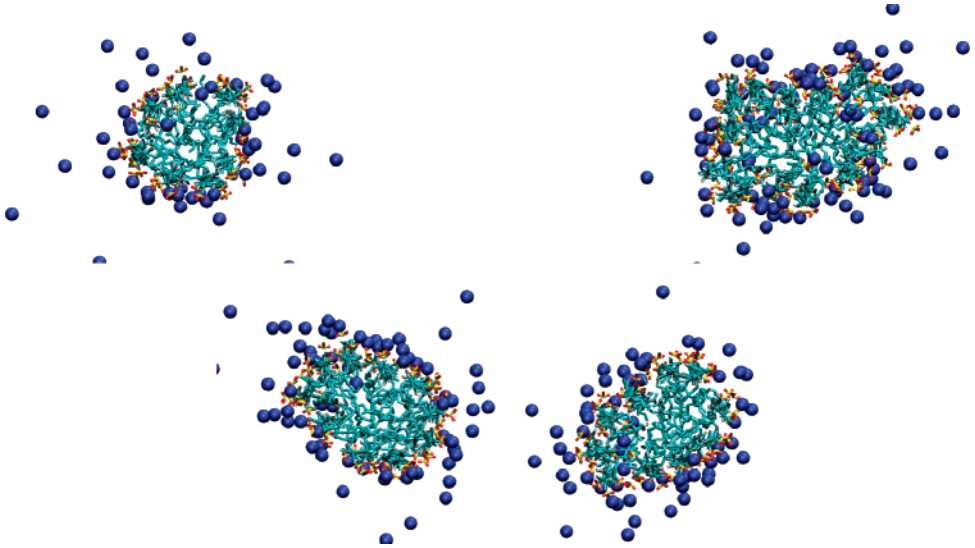

Figure 2. Top view of bundles of size $N = 8$ (top left), $N = 14$ (top right), and $N = 20$ (bottom) oligomers with Na^+ counterions (blue).

finite, if the counterions cannot penetrate into the droplet. However, if counterions are allowed to penetrate, this leads to either finite or infinite droplet sizes, depending on the parameters.

In this study, we analyze the differences in the packing of PPP oligomers with monovalent Na^+ and divalent Ca^{2+} counterions. Furthermore, we propose a possible explanation for the abrupt increase in size upon change of counterion valency and try to validate this with our simulation results.

II. Model and Method

Observing the self-organization of PPP oligomers into cylindrical micelles with explicit water is computationally not feasible. In order to reduce the size of the system and the computational cost, the basic oligomer for the computational model is chosen as four repeat units of the synthetic PPP monomer. Additional test runs with more PPP monomers showed that the results do not depend on the chosen length. In the model PPP oligomer, the order of the side groups and the attachment of the SO_3^- groups are the same for every polymer unit, whereas the aliphatic side chain can be connected to either one of carbons. Periodic boundary conditions are used to mimic an infinitely long polymer along the *z*-axis. This means end effects are ignored. We do not expect end effects to play a significant role on the shape of the cross section, since in the experiments the length of the bundle is several orders of magnitude larger than its cross section.

In the initial setup the PPP oligomers are arranged parallel to the *z*-axis, such that the hydrophobic side chains are packed inside the cylindrical core and the charged groups are located on the outer surface of the cylinder. In order to reduce the electrostatic repulsion of the charged groups, each PPP is shifted along the *z*-axis in the initial conformation, so that the charged groups form a helical pattern. The neutralizing counterions are placed next to the SO_3^- groups. This helical pattern is lost during the simulation and does not influence the results. This preformed bundle is energy minimized before the solvent molecules are added. First, the backbone is fixed, and the side chains and counterions are relaxed. Next the backbones are thermalized, while keeping the terminal carbon atom of the side chains fixed to preserve the cylindrical cross section. After the bundle is equilibrated, water is added in a unit cell that has a hexagonal cross section in the $x-y$ plane. The amount of water is 1000 molecules per polymer, which results in a periodic image distance ranging from 8 nm for 8 PPP oligomers to 15 nm for 30 PPP oligomers, while the height is always 5 nm. The water molecules are excluded from the hydrophobic core region of the bundle during the system setup. After energy minimization of the bundle with the solvent, molecular dynamics simulations with lengths ranging from 15 to 100 ns are performed. The polymers relax to a (meta)stable configuration within 1 ns. The counterion distribution takes somewhat longer to equilibrate; therefore, we excluded at least the first 5 ns of each simulation from the analysis.

For the molecular dynamics simulations the GROMOS 45A3 force field[16] was used. For PPP, this force field does not have parameters for the dihedral angle between two consecutive rings. To obtain the correct twist between the rings (30°) as well as persistence length (10 nm), we had to increase the partial charges on the C and H atoms to ± 0.12 and use a dihedral potential between two rings with minima at 0 and 180° and a force constant of 12 kJ/(mol rad). For the SO_3^- group we used the GROMOS sulfur and charged carboxyl oxygen Lennard-Jones parameters. The charges for sulfur and oxygen were chosen as $1.16e$ and $-0.68e$, respectively. The SPC[17] water model was used, of which the geometry was fixed with the SETTLE algorithm.[18] All bond lengths in the polymers where constrained with the LINCS algorithm.[19] A time step of 4 fs was used. The electrostatics were treated with the particle-mesh Ewald method,[20] with a direct-space cutoff of 0.9 nm and a grid spacing of 0.12 nm. The neighborlist of 0.9 nm as well as the Lennard-Jones interactions between 0.9 and the cutoff of 1.4 nm were updated every five steps. The temperature and pressure were held at 300 K and 1 bar, respectively, using the weak coupling method.[21] All simulations were performed with the Gromacs 3.3 package.[22]

III. Results and Discussion

We will start the analysis of the molecular dynamics data by looking at the equilibrium snapshots of different PPP bundles. Using our computational model for the PPP bundles, we have performed simulations for $N = 8$, 9, 10, 12, 14, 16, and 20 oligomer bundles, where N is the radial aggregation number for the preformed bundle. In Figure 2, snapshots of aggregates of $N = 8$, 14, and 20 from the equilibrated system are shown. These snapshots (as well as the snapshots for the system with Ca^{2+} shown below) are taken at 10, 10, and 100 ns for $N = 8$, 14, and 20, respectively. Note that the water molecules are not shown for clarity. The expected packing mechanism is verified

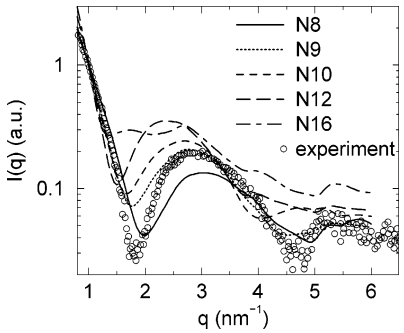

Figure 3. Computed and experimental[23] SAXS intensities. The small aggregates with N between 8 and 10 yield the closest match to the experimental data.

by these equilibrium top view snapshots of the bundles. The hydrophobic side chains remain in the cylindrical core, and the charged groups remain in the outer shell. The Na^+ ions condense onto the bundle, but they do not form permanent dipolar couples with the SO_3^- group, but rather they are free to explore the shell around the cylinder.

As N is increased, the cross section of the bundle increases, which enables the system to reduce its electrostatic self-energy. Two different relaxation mechanisms can be observed. First, the cross section is distorted toward an elliptic shape. Second, penetration of Na^+ ions helps to reduce the repulsive electrostatic interactions between the charged PPP backbones. The Na^+ counterions carry their hydration shell as they penetrate into the hydrophobic core, which is definitely not favored by the water molecules. As can been seen in Figure 2, the counterions in the core remain close to the SO_3^- groups and do not move to the center of the bundle. Already for $N = 14$, the hydrophobic core is heavily invaded by counterions and is highly perturbed. Eventually at $N = 20$, the unfavorable contacts between the hydrophobic side chains and the hydration shells of the Na^+ ions overcome the barrier for opening up the core. As a result, the initial 20 oligomer bundle splits up to form two separate bundles, each one of size $N = 10$ oligomers. After the split, most of the counterions are driven out of the hydrophobic core, and a small fraction of counterions are released in to the solution, decreasing the free energy of the system.

One can compare the small-angle X-ray scattering from the bundles obtained via molecular dynamics simulations with the experimental data which is available only for the Na^+ counterions (Figure 3). These data were produced as follows. First, the electron density ρ of the whole system, including counterions and water, was mapped on a cubic grid with a spacing of 0.25 nm. The electrons, which were assumed to be at the positions of the nuclei of the atoms, were mapped to the eight neighboring grid points using a linear spreading function in each dimension. This procedure is accurate enough for the wavelengths of interest, which are longer than 1 nm. Then summing over all pairs of grid points $i-j$, including periodicity in the z-direction, we determined the scattering intensity:

$$I(q) = \sum_i \sum_j (\rho_i - \rho_w)(\rho_j - \rho_w) \frac{\sin(qr_{ij})}{qr_{ij}} s(r_{ij}) \qquad (1)$$

where ρ_w is the electron density of bulk water. The switching function s is applied to approximate a finite rod:

$$s(r) = \begin{cases} \frac{1}{2} + \frac{1}{2}\cos\left(\frac{\pi r}{r_c}\right) & r < r_c \\ 0 & r \geq r_c \end{cases} \qquad (2)$$

where a distance r_c of 23 nm was used. As long as it is smooth, the choice of switching function has little influence on the results. The data in Figure 3 are normalized to the experimental intensity at $q = 1$ nm^{-1}. For $q > 4$ nm $^{-1}$ the results are somewhat sensitive to the grid spacing. The shape of the experimental curve is typical for a cylindrical rod. The q-spacing of the maxima and minima is set by the diameter of the rod, while the depth of the minima is related to radial symmetry of the rod. The $N = 9$ PPP bundle shows the closest match to the experimental data. It reproduces not only the locations of the two minima but also the height of the maximum at $q = 2.8$ nm^{-1}. This size of nine oligomers is on the lower end of the experimental prediction for PPP bundles with Na^+ as a counterion. The $N = 16$ PPP bundle has a banana-shaped cross section, which causes a complete loss of the first minimum in the scattering curve.

Next, let us look at the PPP bundles with Ca^{2+} counterions, where the experimental data suggest a dramatic increase for the number of oligomers in the cross section from 10 to 60. Equilibrium snapshots for bundles with divalent Ca^{2+} counterions show that the basic packing mechanism does not change (Figure 4). Snapshots for $N = 8$ and $N = 14$ oligomers show no significant difference in terms of the packing of the PPP oligomers due to the exchange of Na^+ with Ca^{2+}. One significant change is the much stronger binding of the divalent counterions due to increased binding energy (Figure 5). Also, the stronger binding of Ca^{2+} seems to reduce the electrostatic self-energy of the bundle to such an extent that the bundles are stable even without counterion penetration in to the hydrophobic core. The picture changes for $N = 20$ oligomers, where the system with Ca^{2+} still remains as a connected single bundle over the simulation time of 100 ns. Two core regions are observed; however, these cores are not completely separated but connected by several side chains.

With monovalent ions a significant number of counterions remain free in solution, and the PPP bundles have a net charge. However, as can be seen in Figure 5 with divalent Ca^{2+} nearly all the counterions stick to the bundle, thereby reducing its net charge to zero. These results for the $N = 10$ bundle are also valid for other bundle sizes investigated in this study. As a result, with the monovalent Na^+ when the $N = 20$ bundle forms two segregated cores with only a few connecting chains, there are strong electrostatic repulsive forces which lead to complete splitting. This net charge creates a sufficiently strong repulsion to overcome the energy barrier for completely breaking the side-chain bridges in between the cores. However, for Ca^{2+} the bundle is almost charge neutral, and therefore there is no strong electrostatic repulsion to push the two 10-PPP cores away from each other. As a result, these 10-PPP cores remain connected via side chains. Furthermore, the multivalent counterion correlations due to Ca^{2+} ions in between the two cores produce an additional gluing force. In other words, the electrostatic forces which are repulsive among bundles for monovalent Na^+ become attractive for Ca^{2+}.

The change in the bundle cross section upon increase of the number of PPP oligomers in the bundle is shown in Figure 6. The radii R_{gi} are the 2D radii of gyration:

$$R_{gi} = \left[\frac{\sum_{j=1}^{N} m_j (\mathbf{r}_j \cdot \mathbf{n}_i)^2}{\sum_{j=1}^{N} m_j} \right]^{1/2}$$

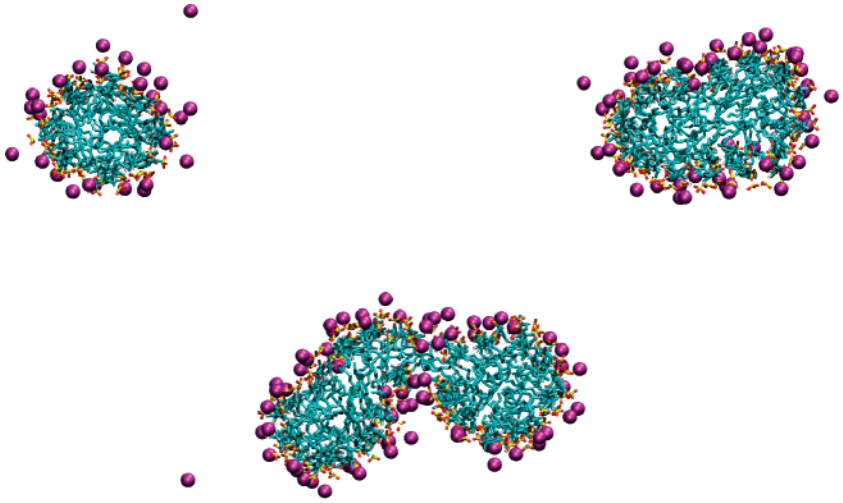

Figure 4. Top view of bundles of size $N = 8$ (top left), $N = 14$ (top right), and $N = 20$ (bottom) oligomers with Ca^{2+} counterions (magenta).

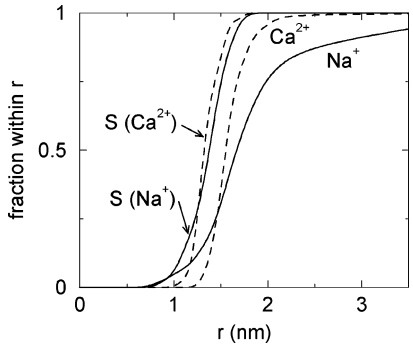

Figure 5. Integrated sulfur and counterion distribution curves as a function of the distance from the center of the bundle for Na^+ (solid lines) and Ca^{2+} (dashed lines) for the 10-PPP aggregate. Unlike the Na^+ counterions, Ca^{2+} remains tightly bound to the outside of the bundle.

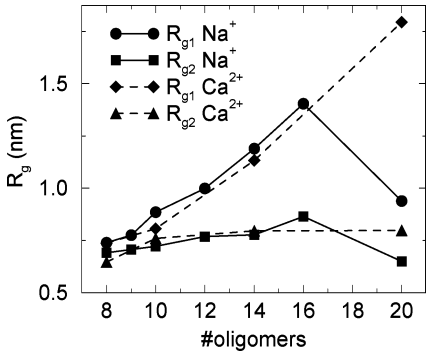

Figure 6. Major and minor radius R_{g1} and R_{g2} of the cross section of the PPP bundles. The minor radius is determined by the side-chain length. The major radius increases with increasing oligomer number. No significant dependence on the counterion valency.

where m_j is the mass and $\mathbf{r}_j$ is the distance of atom j from the center of the bundle and $\mathbf{n}_1$ and $\mathbf{n}_2$ are the directions of the major and minor axis. The minor radius, which is mainly set by the length of the hydrophobic side chains, remains almost constant. On the other hand, the major radius increases linearly as a function of the number of oligomers in the bundle. The flat shape of the larger bundles is the only option for screening all the side chains from the solvent, while keeping the charged groups in contact with the solvent. For the Na^+ counterion case, the major radius drops at $N = 20$ since the system splits up to form two separate bundles.

A simulation of a 30-PPP bundle composed of charge neutral PPP oligomers has shown that, in the absence of electrostatic repulsive forces, the bundle remains intact, as one big aggregate. The neutral PPP oligomers were obtained by increasing the sulfur charge by 1*e*, so that these groups are charge neutral but still polar. Furthermore, all counterions are removed from the solution. In the absence of long-range electrostatic forces, there is no force counteracting the hydrophobic attractive forces. The two radii of the charge neutral PPP bundle are 1.6 and 1.0 nm. The minor radius is larger than the characteristic minor radius observed for both Na^+ and Ca^{2+}. This in silico experiment proves that the amphiphilic nature of the polymers is not sufficient to limit the aggregate size but that charged groups are required.

IV. Conclusions

The simulation results demonstrate the stability of cylindrical micelles in agreement with the experimental results. The basic packing of the hydrophobic side chains in the core of the cylindrical aggregate is validated. This hydrophobic core is free of water for stable aggregates. However, in order to reduce the electrostatic energy, a small fraction of counterions can penetrate into this hydrophobic core, especially for the monovalent Na^+ case. Penetration of counterions with their hydration shells leads to destabilization of the hydrophobic core and has a significant contribution in determining the size of the bundles. When divalent Ca^{2+} counterions are used, the core is not disturbed and the micelles are highly ordered. However, with multivalent ions the bundle−bundle interactions shift from repulsive to attractive. This sign change in the effective interaction could lead to formation of bundles of bundles, which could explain the 60-PPP aggregates observed in experiment. One might ask what the size limiting mechanism for this bundle of bundles is. In a recent study[8] we have shown that even in the presence of only electrostatic interactions, one can still obtain a finite size aggregate at thermodynamic equilibrium. This finite size is stabilized by the finite size of the systems as well as the counterion entropy.

Acknowledgment. We thank the EC for providing a Marie Curie Intra-European Postdoctoral Fellowship to M. Sayar (MCIEF 500604). Additional funding from the DFG through Grant SFB 625 and Ho1108/11-3 is gratefully acknowledged. We thank M. Deserno, N. van der Vegt, and K. Kremer for stimulating scientific discussions and G. Wegner and A. Kröger for discussions on the interpretation of the experimental results.

References and Notes

(1) Grosberg, A. Y.; Nguyen, T. T.; Shklovskii, B. I. *Rev. Mod. Phys.* **2002**, *74*, 329.
(2) Levin, Y. *Rep. Prog. Phys.* **2002**, *65*, 1577−1632.
(3) Holm, C., Kékicheff, P., Podgornik, R., Eds. *Electrostatic Effects in Soft Matter and Biophysics; NATO Sci. Ser. II: Mathematics, Physics and Chemistry*; Kluwer Academic Publishers: Dordrecht, 2001; Vol. 46.
(4) Boroudjerdi, H.; Kim, Y.-W.; Naji, A.; Netz, R. R.; Schlagberger, X.; Serr, A. *Phys. Rep.* **2005**, *416*, 129−199.
(5) Bloomfield, V. *Biopolymers* **1991**, *31*, 1471.
(6) Tang, J. X.; Wong, S.; Tran, P. T.; Janmey, P. *Ber. Bunsen-Ges. Phys. Chem.* **1996**, *100*, 796−806.
(7) Käs, J.; Strey, H.; Tang, J.; Finger, D.; Ezzell, R.; Sackmann, E.; Janmey, P. *Biophys. J.* **1996**, *70*, 609−625.
(8) Sayar, M.; Holm, C. *Europhys. Lett.* **2007**, *77*, 16001.
(9) Bockstaller, M.; Köhler, W.; Wegner, G.; Vlassopoulos, D.; Fytas, G. *Macromolecules* **2000**, *33*, 3951−3953.
(10) Kroeger, A.; Deimede, V.; Belack, J.; Lieberwirth, I.; Fytas, G.; Wegner, G. *Macromolecules* **2007**, *40*, 105−115.
(11) Kroeger, A.; Belack, J.; Larsen, A.; Fytas, G.; Wegner, G. *Macromolecules* **2006**, *39*, 7098−7106.
(12) Limbach, H. J.; Sayar, M.; Holm, C. *J. Phys.: Condens. Matter* **2004**, *16*, S2135−S2144.
(13) Limbach, H. J.; Holm, C.; Kremer, K. *Macromol. Chem. Phys.* **2005**, *206*, 77−82.
(14) Deserno, M. *Eur. Phys. J. E* **2001**, *6*, 163−168.
(15) Tamashiro, M.; Schiessel, H. *Phys. Rev. E* **2006**, *74*, 021412.
(16) Schuler, L. D.; Daura, X.; van Gunsteren, W. F. *J. Comput. Chem.* **2001**, *22*, 1205−1218.
(17) Berendsen, H. J. C.; Postma, J. P. M.; van Gunsteren, W. F.; Hermans, J. Interaction Models for Water in Relation to Protein Hydration. In *Intermolecular Forces*; Pullman, B., Ed.; D. Reidel Publishing Co.: Dordrecht, 1981.
(18) Miyamoto, S.; Kollman, P. A. *J. Comput. Chem.* **1992**, *13*, 952−962.
(19) Hess, B.; Bekker, H.; Berendsen, H. J. C.; Fraaije, J. G. E. M. *J. Comput. Chem.* **1997**, *18*, 1463−1472.
(20) Essmann, U.; Perera, L.; Berkowitz, M. L.; Darden, T.; Lee, H.; Pedersen, L. G. *J. Chem. Phys.* **1995**, *103*, 8577−8592.
(21) Berendsen, H. J. C.; Postma, J. P. M.; van Gunsteren, W. F.; DiNola, A.; Haak, J. R. *J. Chem. Phys.* **1984**, *81*, 3684−3690.
(22) van der Spoel, D.; Lindahl, E.; Hess, B.; Groenhof, G.; Mark, A. E.; Berendsen, H. J. C. *J. Comput. Chem.* **2005**, *26*, 1701−1718.
(23) Bockstaller, M.; Köhler, W.; Wegner, G.; Fytas, G. *Macromolecules* **2001**, *34*, 6353−6358.

MA062624G